

Synthesis and Mass Spectrometric Characterization of a Metal-Affinity Decapeptide: Copper-Induced Conformational Changes

Manuela Murariu,[†] Ecaterina Stela Dragan,^{*,†} and Gabi Drochioiu^{*,‡}

"Petru Poni" Institute of Macromolecular Chemistry, Aleea Grigore Ghica Voda 41 A, RO-700487 Iasi, Romania, and Faculty of Chemistry, "Al. I. Cuza" University of Iasi, 11 Carol I, RO-700506 Iasi, Romania

Received July 18, 2007; Revised Manuscript Received September 14, 2007

A decapeptide with high affinity toward heavy metal ions (RCHQYHHNRE) has been prepared by Fmoc strategy using TGR resin as solid support. The model peptide provides a simple system that can be used for a systematic study of the impact of different metal ions on peptide secondary structure on a molecular level; histidine residues were incorporated into the peptide in a sequence similar to beta-amyloid peptide (A β 1–40) to generate possible complexation sites for Cu²⁺ ions. The peptide secondary structure, as investigated by circular dichroism, and self-assembled nanostructures were observed to depend strongly on the presence of copper and sodium dodecyl sulfate (SDS). Atomic force microscopy (AFM) revealed also that copper and SDS affected slightly the A β 1–40 nanostructures. An explanation for the effect of metal ions and SDS on the self-assembly of peptides was proposed. The extensive β -sheet formation may further promote peptide self-assembly into longer fibers.

I. Introduction

Peptide synthesis has become one of the most important methodologies in bioorganic and biomacromolecular chemistry.^{1–7} Synthetic peptides and their metal complexes are of paramount importance for the understanding of the biochemical and pathophysiological processes within the living bodies. They have various applications for analytical purposes: in medical practice as biofilms and hybrid copolymers for drug release, in the decontaminating hazardous heavy and radioactive materials, and so on.^{2,8–11} New biologically active peptides continue to be discovered that exhibit remarkable diverse functionalities and include antibiotics, toxins, immunosuppressants, ion transport regulators, inhibitors of protein binding, enzyme inhibitors, and so on.¹² Metal-based reactions of some polypeptides and proteins are considered as a common denominator for neurodegenerative diseases.¹³ For example, one of the main neuropathological features of the Alzheimer's disease (AD) brain are the extracellular amyloid deposits consisting of fibrils of β -amyloid peptide,¹⁴ associated with lipids, metal ions, and other proteins. In addition, the transformation process from α -helices to β -sheet structures appears to be one of the major factors in the genesis and evolution of a variety of neurodegenerative diseases such as AD, Parkinson's disease, and several prion diseases.^{15–17} Studies with the beta-amyloid peptide (A β 1–40) show that apolipoprotein E (apoE) and serum amyloid P (SAP) promote A β 1–40 fibril formation,^{18,19} whereas other works show that apoE and SAP inhibit A β 1–40 fibril formation.^{20,21} Copper ions cause the peptide to aggregate to a great extent and markedly increase the neurotoxicity exhibited by A β 1–40 in cell culture.²² Some novel analytical methods have been used to characterize peptides and their complexes, as well as their conformational transformations. Electrospray ionization (ESI) mass spectrometry shows that copper binds to A β 1–16²² at pH 6.0 and 7.0. The

mode of copper binding is highly pH-dependent.⁸ Atomic force microscopy (AFM) is a relatively new imaging technique with nanomolar resolution on soft biological macromolecules.^{6,7,23} AFM offers the capability for measuring individual molecules or self-assembling peptides and providing high resolution structural information.²⁴ Solid phase peptide synthesis (SPPS), as developed by R. B. Merrifield,²⁵ proved to be a powerful tool for producing peptides, and various peptides were easily synthesized by the Fmoc methodology²⁶ using TGR resin. Biology and medicine are beginning to reduce the problems of disease to problems of molecular science and are creating new opportunities for treating and curing disease. Such advances are coupled closely with advances in biomaterials and are leading to a variety of approaches for relieving suffering and prolonging life.²⁷ The ability to look at individual molecules has given us new insights into molecular processes in biology.²⁸

Therefore, the auspicious structural and pathophysiological alterations of copper-dependent fibril-forming polypeptides prompted us to synthesize a RCHQYHHNRE (Arg-Cys-His-Gln-Tyr-His-His-Asn-Arg-Glu) decapeptide with specific metal binding properties. The decapeptide was characterized by circular dichroism (CD), mass spectrometry, and AFM and compared with the data obtained for the synthetic A β 1–40 peptide, which plays an important pathophysiological role in the neurodegenerative diseases.

II. Experimental Section

II.1. Materials. NovaSyn TGR resin was purchased from Nova-biochem. Protected amino acids for peptide synthesis were provided by GL Biochem (Shanghai, China). All solvents for peptide synthesis were commercially analytical grade and were redistilled before use. Dimethylformamide (DMF), piperidine, and 4-methylmorpholine were purchased from Sigma, and bromophenol blue, ninhydrine, acetonitrile, and trifluoroacetic acid (TFA) were purchased from Merck. A β 1–40 with the following sequence H-DAEFRHDSGYEVHHQKLFFFAED-VGSNKGAIIGLMVGGVV-NH₂ was manually synthesized, by SPPS, according to the Boc/Bzl strategy using 4-methylbenzhydrylamine resin (MBHA resin; capacity of 0.5 mmol/g) as a support.²⁵

* Corresponding author. Tel.: +40.2322217454 (E.S.D.); +40.232201278 (G.D.). Fax: +40.232211299 (E.S.D.); +40.232201313 (G.D.).

[†] "Petru Poni" Institute of Macromolecular Chemistry.

[‡] "Al. I. Cuza" University of Iasi.

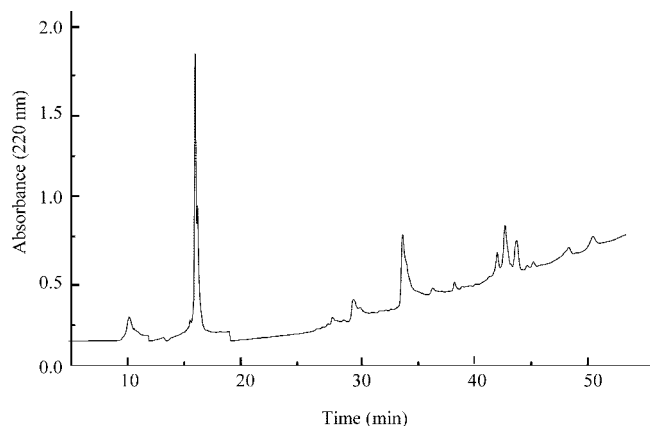


Figure 1. Analytical RP-HPLC of crude decapeptide. The peptide eluted at 16.52 min on a Spherisorb C18 column, with a gradient of 10–60% solvent B in solvent A, at 1 mL/min.

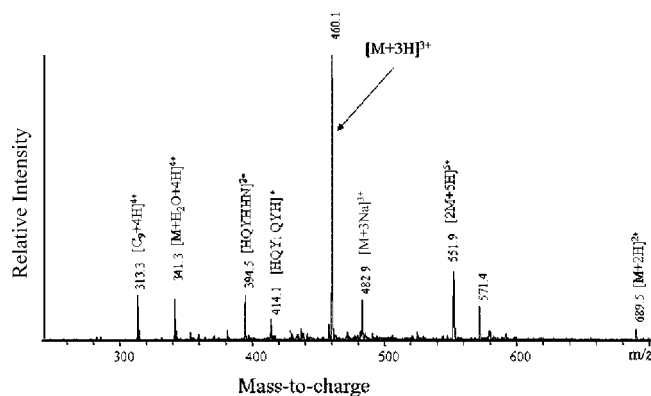


Figure 2. ESI ion trap MS spectrum of the peptide RCHQYHHNRE and its fragments.

II.2. Synthesis of Decapeptide. Attachment of the first amino acid to resin is still a serious problem.²⁶ Therefore, we used TGR resin with the preloaded first amino acid. The peptide was prepared manually by the classic Fmoc methodology using the TGR resin as solid support in a glass reaction vessel (30 mL) fitted with a sintered glass frit. Side chain protecting groups included 2,2,4,6,7-pentamethyldihydrobenzofurane (Pbf) for Arg, trityl (Trt) for Asn, Cys, and His, and *t*-butyl (*t*-Bu) for Tyr and Gln. Solvent and soluble reagents were removed by suction. Washings steps of resin were performed with dichloromethane (DCM), ethanol (EtOH), and DMF (each with 5 mL, 3 × 2 min).

II.2.1. Formation of Amide Bonds. The Fmoc-amino-acids, Fmoc-Arg(Pbf)-OH, Fmoc-Asn(Trt)-OH, Fmoc-His(Trt)-OH, Fmoc-Tyr(*t*-Bu)-OH, Fmoc-Gln(Trt)-OH, and Fmoc-Cys(Trt)-OH, were attached to the resin one by one using *N*-methylmorpholine as the coupling reagent. After Fmoc-Arg(Pbf)-OH (0.329 g) was preactivated using PyBOP (benzotriazol-1-yl-*N*-oxytripyrrolidinophosphonium hexafluorophosphate; 0.20 g), 100 μ L of *N*-methylmorpholine dissolved in the smallest amount of DMF was poured into the resin. The coupling reaction mixture was incubated for 1 h at room temperature, being verified by the ninhydrin (Kaiser) test.²⁶ The double coupling process was performed under the same conditions when the ninhydrin test was positive. After washing the resin, the Fmoc group was removed by piperidine/DMF (20%) as above-mentioned. Then, the coupling procedures of the other Fmoc-amino acids were similarly performed.

II.2.2. Cleavage of Peptides from Resin. After the final step of deprotection of the Fmoc group, the obtained resin bound peptide was dried in vacuo and treated with trifluoroacetic acid (TFA)/H₂O/triethylsilane (TES; 90/5/5, v/v) for 3 h to cleave the peptide from the resin and remove the side chain protecting groups. The resin was filtered and the filtrant was washed several times with diethylether and then lyophilized after peptide extraction with 5% acetic acid solution.

In another synthesis procedure, we passed over the final deprotection with piperidine of the peptide bound to resin in order to obtain the Fmoc-protected decapeptide. The resulted Fmoc-decapeptide was used to investigate the metal ion binding to amino acid residues only.

II.2.3. Peptide Characterization Program. A GPWAW 6.10 (General Protein/Mass Analysis for Windows, Lighthouse Data, Denmark) program was used for the calculation of the monoisotopic and average masses of the peptides, the MS/MS fragmentation, and the hydrophobicity of a given peptide sequence.

II.3. Chromatography. A BIO-RAD Model 2700Elite RP-HPLC system (Bio-Rad Laboratories GmbH, Germany), using a Spherisorb (ODS) C18 reversed-phase analytical column, was used for the purification of the decapeptide. The peptide (1 mg) was dissolved in 1 mL of acetonitrile/water (80:20, v/v containing 0.1% TFA), filtered using a filter funnel G4, and manually injected through an injector with a 10 μ L sample loop. A mixture of two solutions was used as the mobile phase: eluent A, 0.1% aqueous TFA; and eluent B, 0.1% TFA in acetonitrile–water (4/1, v/v), with a flow-rate of 1 mL/min. The column was washed with 5% B and 95% A for 5 min, and the peptide was eluted using a linear gradient of 5–45% B for 40 min, with a flow rate of 1 mL/min.

Analytical RP-HPLC for the A β 1–40, which is a hydrophobic peptide, was performed on a Knauer system (H. Knauer, Bad Homburg, Germany) using an analytical Phenomenex Jupiter C4 column (250 × 4.6 mm I.D.), with 5 μ m silica (Torrance, CA) as a stationary phase. Linear gradient elution (0 min 0% B; 5 min 0% B; 55 min 100% B) with eluent A and eluent B was used at a flow rate of 1 mL/min at ambient temperature. Eluted products were detected at 220 nm.

II.4. Mass Spectrometry. Both a matrix-assisted laser desorption/ionization time-of-flight (MALDI-TOF Finnigan MAT LASERMAT 5000) spectrometer and an ion trap Esquire 3000 Plus spectrometer (Bruker Daltonics, Bremen, Germany) were used to determine the masses of peptides and their metal complexes.

II.4.1. MALDI-TOF Measurements. The MALDI-TOF was equipped with a nitrogen UV laser ($\lambda_{\text{max}} = 337$ nm). For each measurement, 1 μ L of a freshly prepared saturated solution of α -cyano-4-hydroxycinnamic acid in acetonitrile/0.1% TFA (2:1 v/v) was applied onto the dry stainless steel MALDI target, and 1 μ L of the sample solution was added and allowed to dry. Acquisition of spectra was carried out at an acceleration voltage of 20 kV and a detector voltage of 1.5 kV. Fifty single shoots were accumulated into a final spectrum. External calibration was carried out using the average masses of single protonated ion signals of bovine insulin (5734.5 Da), oxidized bovine insulin β -chain, (3496.9 Da), bee venom melittin (2847.5 Da), human adrenocorticotrophic hormone (ACTH) fragment (2466.7 Da), human neurotensin (1673.9 Da), human angiotensin I (1297.5 Da), human bradykinin (1061.2 Da), and human angiotensin II (1047.2 Da).

II.4.2. Electrospray Ionization–Ion Trap Mass Spectrometry. Spectra were acquired in the 50–2000 m/z range. Samples were dissolved in acetonitrile–water (1:1, v/v) solvent mixture, containing 0.1% acetic acid. Binding of metal ions to β -amyloid peptides was studied by ESI-ion trap MS using 5 mM ammonium acetate, pH 6.6, as a solvent. Peptide concentration was 10 pmol/ μ L, and the ratios of peptide/metal ion were 1:1, 1:2, and 1:10. Before complexation, the A β 1–40 peptide and CuSO₄ were separately dissolved in 5 mM ammonium acetate and mixed to form complexes prior to MS analysis.

II.5. CD Spectropolarimetry. CD spectra were recorded using a Spectropolarimeter (Labor and Datentechnik GmbH, Germany) equipped with thermal circulator accessory and spectrometer software (Dr. Jrg Nerkamp). All measurements were performed in quartz cells with a path length of 0.5 mm. Data were collected at the wavelengths from 180 to 280 nm in 0.2 nm increments. Six individual data were averaged by device in order to obtain the reported CD spectrum. The measurements were carried out at 25.0 \pm 0.2 $^{\circ}$ C.

II.6. AFM. AFM has the potential to monitor structural changes of individual molecules. Nanostructures formed by self-assembly of the peptides in pure water and the sodium dodecyl sulfate (SDS) and GdV

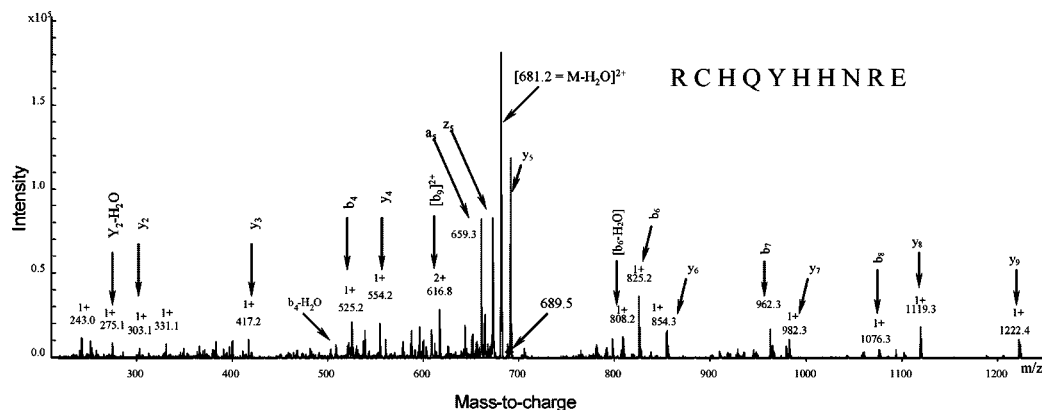


Figure 3. MS/MS spectrum of the double-charged RCHQYHHNRE decapeptide (m/z 689.5) confirmed the peptide sequence.

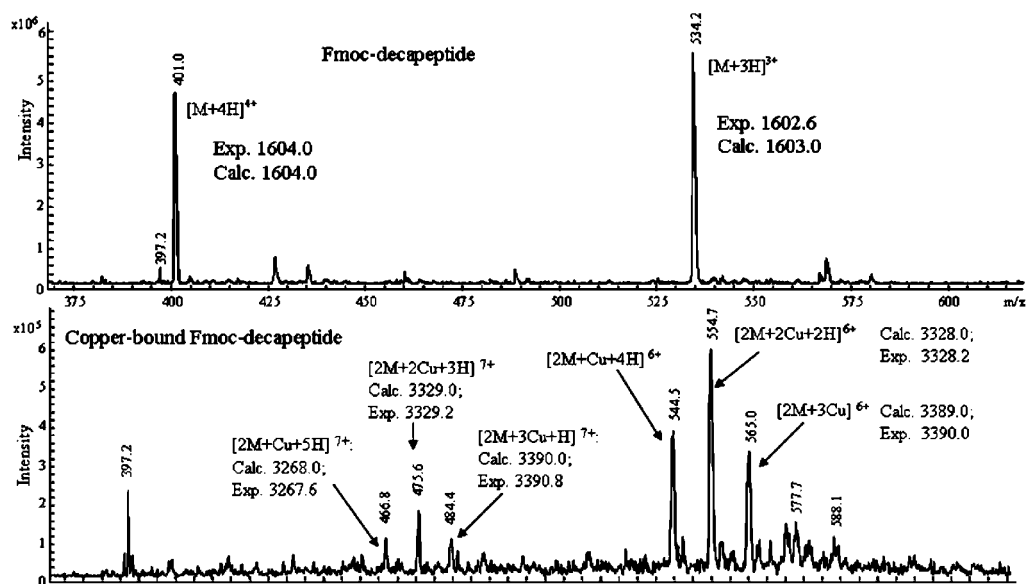


Figure 4. ESI ion trap MS spectra of Fmoc-decapeptide and its complex with copper ions.

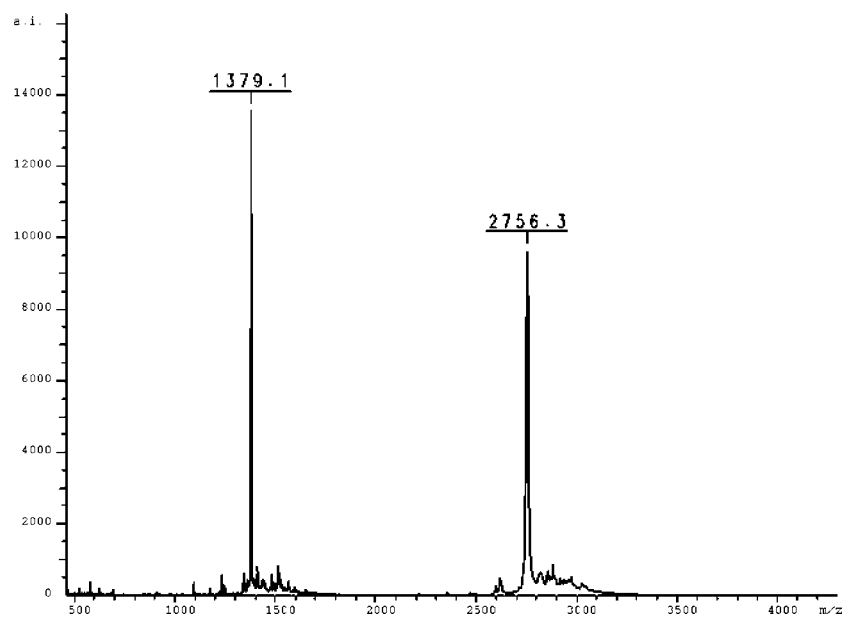


Figure 5. MALDI-ToF MS spectrum of decapeptide, in which both oxidized and reduced forms appeared.

copper salt solutions were characterized by AFM. Approximately 50 μ L of sample solution was placed on the microscope glass plate, covered by a Petri-dish to avoid dust, and allowed to dry overnight. Images were taken at room temperature (22 $^{\circ}$ C) on a SPM Solver PRO-M

AFM (NT-MTD Co. Zelenograd, Moscow, Russia) using the tapping mode. This mode was used to reduce sample surface distortion due to tip and sample interactions. All images were acquired using a high resolution noncontact "Golden" silicon NSG10/Au/50 cantilever with

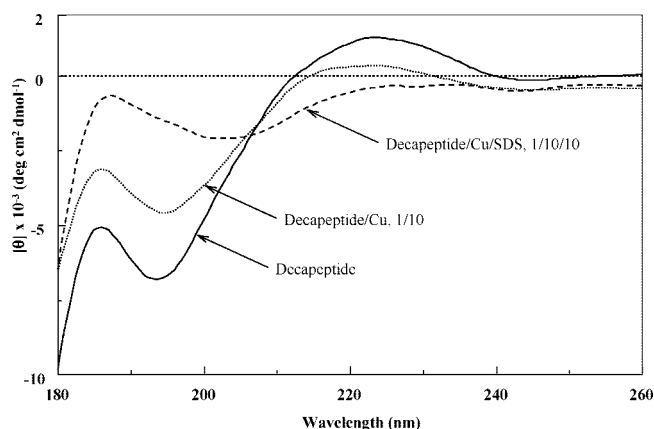


Figure 6. CD spectra of the reduced form of decapeptide in the presence of copper ions and sodium dodecyl sulfate (SDS): decapeptide concentration, 0.7 mM; concentration of copper ions and SDS, 7 mM.

Au conductive coating. The cantilever was 100 μm in length, 35 μm in width, and with a 2 μm thickness and had a typical tip radius of 10 nm. A resonant frequency of 254 kHz and a force constant of 11.5 N/m were applied. All AFM images were obtained at a resolution of 256×256 pixels on a scale of $10 \mu\text{m} \times 10 \mu\text{m}$. Image analysis was done with scanning probe microscopy software, WSxM 4.0 Develop 10.0 (Nanotec Electronica S. L.).

III. Results and Discussion

To study the influence of metal ions on the secondary structure of the peptides, we introduced three histidine residues per molecule of decapeptide as binding sites for metal ions. This sequence is rather similar to that in A β 1–40 peptide. Therefore, histidine residues were placed within the peptide molecule, such that an efficient complexation of metal ions happen in the case of β -sheet formation. It is generally accepted that SH-peptides also bind heavy metal ions, which prompted us to include a cysteine residue in our decapeptide primary sequence.

III.1. Synthesis and Characterization of Decapeptides. The resulted amount of crude decapeptide was 146.4 mg, with a 5% higher than the minimum resin loading capacity. Analytical RP-HPLC of the crude peptide (Figure 1) showed one major component eluting at 16.52 min along with a few other components. However, the peptide eluting at 16.52 min was a mixture of the reduced form with a small amount of the oxidized one (less than 5%). The equilibrium was shifted to the reduced form of the decapeptide at 90 $^{\circ}\text{C}$ for 30 min by using dithiothreitol as reducing agent. The reduced decapeptide gave the expected ESI ion trap MS $[\text{M} + 3\text{H}]^{3+}$ ion at 460.1 mass units (Figure 2) and $[\text{M} + 2\text{H}]^{2+}$ ion at 689.5 (low peak). Some additional fragments corresponding to this peptide appeared in the spectrum made with the Esquire3000Plus instrument because of the fragmentation process. We calculated the MS/MS fragmentation with the help of the GPMAW program and identified the fragments in the ESI ion trap spectrum. These fragments were not present in the MALDI-ToF MS spectrum and, therefore, we assumed that they were a result of the thermal decomposition of the pure decapeptide.

The perfect combination of collisionally activated decomposition (CAD) technique and electrospray ionization (ESI) in ion trap mass spectrometers accelerated the development of de novo sequencing, which is a highly efficient tool for the determination of the amino acid sequence of synthetic or natural peptides.²⁹

Sequencing peptides by tandem mass spectrometry (MS/MS) has some distinct advantages when compared with Edman degradation.³⁰ Therefore, we selected a single double-charged decapeptide with m/z 689.5 from the peptide mixture without further purification and sequenced it by the mass-selection function of the instrument. The sample amount necessary for analysis was usually less than 1 pmol to acquire a high quality mass spectrum, which provides the molecular weight as well as the purity. Because the experiment operation is noticeably simplified, sequence elucidation by MS/MS is very suitable for analyzing a synthetically crude peptide.³¹ Applying this procedure, we clearly confirmed the primary structure of the investigated peptide from a mixture of peptides, peptide fragments, and nonproteic molecules (Figure 3). Under the experimental conditions, the double-charged molecule of decapeptide generated both small and large fragments, most of them of y type ($y_2 - y_9$). Some of them, including the molecular ion, lose water to give additional fragments that have been identified with the GPMAW program. Therefore, they were expected to appear due to the splitting of decapeptide molecules in the presence of argon in the MS/MS process.

To minimize copper-amino group interactions and to stabilize the decapeptide in the reduced form, the Fmoc-protected peptide has also been synthesized. It is known that histidine-containing peptides bind copper ions.³² Indeed, the protected peptide showed a high copper-binding capability at the physiological pH value assigned to histidine residues. Knowing the high affinity of the SH group (due to presence of cysteine in the peptide sequence) toward copper ions, we suppose that a copper bridge between two sulfur atoms was formed. To eliminate the amino group contribution to binding copper ions, the Fmoc-protecting group was kept in the peptide sequence (Figure 4). The ESI ion trap MS spectrum showed that the copper binding to peptide resulted in the dimerization of single molecules. In addition, more than one copper ion was bound in the physiological range of pH. The spectrum clearly displayed some complexes formed between two molecules of the peptide and a maximum of three copper ions (Figure 4). In addition, the instrument has some limitations when measuring the spray solutions at higher temperatures than 100 $^{\circ}\text{C}$. Lowering the spray temperature showed the formation of multiple copper-peptide complexes (not shown).

In the presence of oxygen, the peptide is readily oxidized to form a mixture of both reduced and oxidized forms, as shown by MALDI-ToF MS measurement (Figure 5). Both reduced and oxidized forms were investigated by CD and MS in the presence of copper ions or SDS. Copper binding to cysteine and histidine residues changed the conformation of the single peptide molecule.

III.2. CD Study. The influence of the environmental conditions (the presence of metal ions or SDS) on the secondary structure of the peptide was followed by CD spectroscopy. Metal ion complexation has previously been shown to be a strong trigger for a secondary structure switch from an α -helix to a β -sheet.¹⁶ However, the peptides investigated here had a different behavioral pattern, although they significantly changed their conformation. The CD spectra of decapeptide (1 mg/mL, 0.7 mM) in aqueous solutions in the presence of copper ions and SDS are shown in Figure 6. The CD spectrum of pure decapeptide showed a small degree of ordering (57.7% random coil). We should note that this decapeptide was not capable of forming an α -helix conformation because of the short length and amino-acid composition.

Table 1. Conformational Changes of the Reduced Decapeptide (Deca) and β -Amyloid Peptide ($A\beta$ 1–40) in the Presence of Copper Ions (Cu) and Sodium Dodecyl Sulfate (SDS)

conformation (%)	deca	deca/Cu	deca/Cu/SDS	$A\beta$	$A\beta$ /Cu	$A\beta$ /Cu/SDS
α -helix	0.0	0.0	0.0	0.0	2.3	22.8
β -sheet	0.0	10.1	53.8	34.3	36.2	46.0
β -turn	42.3	32.9	6.8	16.6	19.6	0
random coil	57.7	57.1	39.4	49.1	41.9	31.2
total	100.0	100.0	100.0	100.0	100.0	100.0

Conformational changes of the decapeptide in the reduced form as well as $A\beta$ 1–40 in the presence of copper ions and SDS are summarized in Table 1. By addition of copper ions, the conformational equilibrium turned to β -sheet conformations, although the proportion of unordered conformers was unchanged. Copper induced a slow increase in the population of beta conformers, whereas SDS induced a significant decrease of random coil and β -turn proportions and an increase of the β -sheet ones. On adding SDS, the conformational equilibrium changed from unordered and β -turn structures to β -conformers (Table 1, Figure 6).

The addition of 10 moles of Cu^{2+} to 1 mol of peptide had an expected impact on the folding of the peptide, which showed a switch from the mainly β -turn conformation to a secondary structure that was mainly β -sheet, especially when SDS was used. The secondary structure switch can be reversed by simply capturing the β -sheet-stabilizing metal ions and, as a result, can be arbitrarily shifted in either direction.¹⁶ Additionally, the similar behavior of Cu^{2+} indicated that the conformational change was not influenced by oxidative effects.

Conformationally, $A\beta$ 1–40 in the fresh water solutions was found as a mixture of random coil (49.1%), β -sheet (34.3%), and β -turn (16.6%) forms. After 36 h, the content in the β -sheet conformer increased from 34.3% up to 42.4%, while the unordered form decreased from 49.1% down to 42.9%. On adding SDS to an old solution of $A\beta$ 1–40 (after 48 h), unexpected changes in the proportion of conformers were observed. β -Turn conformers disappeared completely (0.0%), whereas α -helix forms increased from 0% up to 36.6%. In the

presence of SDS, the β -sheet content of the peptide remained almost constant, while the unordered forms were found in a smaller proportion (30.7%). The transformation of the unordered conformers into the β -sheet ones determines the self-aggregation and the fibril formation; a larger proportion of conformers in the α -helix form prevent the aggregation of the molecules. Hence, both decapeptide and $A\beta$ 1–40 will form fibrils in the presence of copper ions due to the increase in β -sheet species. Also, the addition of SDS to a copper–decapeptide complex in the solution resulted in the enhancement of the fibrillation process. On the contrary, the addition of SDS to $A\beta$ fibrils, formed in the presence of copper ions, caused their atomization.

III.3. Effect of Copper Ions on the Self-Assembled Peptide Nanostructures. The strong contrast between the AFM images recorded before and after copper treatment confirmed a morphological change in the surface packing of the peptide shell. Our results showed that the self-assembled nanostructures of peptides in aqueous solution were significantly influenced by the presence of copper ions and SDS. Copper favored intermolecular attractions and β -sheet formation in some extent (Table 1). The extensive β -sheet formation may cause the peptides to form long fibers due to the growth in the direction perpendicular to the β -strands or the interaction between β -sheets. AFM produced faithful high-resolution images of peptide surfaces in the aqueous environment (Figure 7).

Figure 7A showed a smooth surface with small peptide nanostructures. On adding copper, the fibril formation as large nanostructures was evident in Figure 7B, although we provided

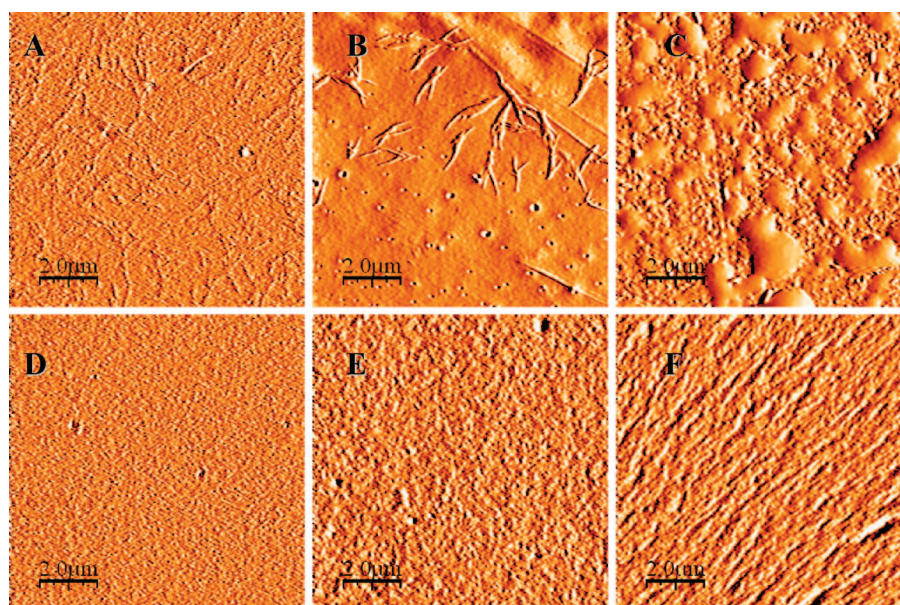


Figure 7. Representative AFM images of decapeptide and $A\beta$ 1–40 peptide: A, the pure decapeptide; B, the decapeptide in the presence of copper ions (1:1 molar ratio); C, the decapeptide in the presence of both copper ions and SDS (1:1:1 molar ratio); D, $A\beta$ 1–40 peptide in pure water; E, $A\beta$ 1–40 peptide in the presence of copper ions; F, $A\beta$ 1–40 peptide in the presence of both copper ions and SDS (1:1:1 molar ratio).

here only the AFM evidence for structural changes. SDS generated large assemblies with a complicated structure (Figure 7C). Some parameters were calculated to quantify the differences between the three images of the decapeptide. For example, root-mean-square roughness for images in Figure 7A–C was 9.22, 8.28, and 2.79 nm, respectively, whereas the average heights were 4.13, 6.87, and 1.29 nm, respectively. On the other hand, the A β 1–40 secondary structure contains mixed random coils and β -sheet in copper solutions. These mixed structures may prevent long fiber formation, causing the peptide to self-assemble to short fibers and small aggregates, similar to that observed in pure water. AFM images of A β 1–40 (Figure 7D–F) were different from those taken for the decapeptide. They showed that the surface becomes rough on adding copper and more structured (“crystallized”) in the presence of SDS.

IV. Conclusions

We have reported here the synthesis of a high metal-affinity decapeptide (RCHQYHHNRE) and its characterization by MS, CD, and AFM techniques. The decapeptide proved to be a useful model for the investigation of copper binding to peptides and to understand the conformational changes induced by metal ions. It was demonstrated that the binding of copper to the peptides plays an important role in the formation of nanostructures. The decapeptide RCHQYHHNRE was compared with the A β 1–40 peptide because of their similarities. Although the decapeptide and A β peptide are rather structurally similar, their copper binding capabilities and conformational changes were significantly different. Copper induced an increase in the population of β -sheet, a slow decrease of β -turn, and an unchanged random coil conformation for decapeptide; both β -sheet and β -turn conformations increased and random coil decreased for the A β 1–40 peptide. However, the α -helix conformation present in A β 1–40 complexes should not be neglected.

Finally, the changes in the nanofibrils obtained, associated with the capability of SDS to control the secondary structure of the peptide associations, make these systems very interesting candidates for understanding related degenerative biochemical processes, as well as the impact of noxious heavy metals in the environment on the living proteome.

Acknowledgment. The authors thank Professor Dr. h.c. Michael Przybylski for his kind advice and Dr. Marilena Manea for the A β 1–40 synthesis. Financial support by Romanian Academy Grant 241/2007 is gratefully acknowledged. G.D. was granted with a 3-month DAAD stipendium to study in Konstanz University in 2007.

References and Notes

- (1) Dijk, M.; Mustafa, K.; Dechesne, A. C.; Nostrum, C. F.; Hennink, W. E.; Rijkers, D. T. S.; Liskamp, R. M. J. *Biomacromolecules* **2007**, *8*, 327–330.
- (2) Drochioiu, G.; Murariu, M.; Petre, B. A.; Manea, M.; Przybylski, M. *Rev. Chim.* **2007**, *58*, 311–315.
- (3) Cardenas, M.; Elofsson, U.; Lindh, L. *Biomacromolecules* **2007**, *8*, 1149–1156.
- (4) Karino, T.; Ikeda, Y.; Yasuda, Y.; Kohjiya, S.; Shibayama, M. *Biomacromolecules* **2007**, *8*, 693–699.
- (5) Kanchanasopa, M.; Manias, F.; Runt, J. *Biomacromolecules* **2003**, *4*, 1203–1213.
- (6) Ikeda, S.; Morris, V. J. *Biomacromolecules* **2002**, *3*, 382–389.
- (7) Camesano, T. A.; Wilkinson, K. J. *Biomacromolecules* **2001**, *2*, 1184–1191.
- (8) Drochioiu, G.; Damoc, E. N.; Przybylski, M. *Talanta* **2006**, *69*, 556–564.
- (9) Popa, K.; Murariu, M.; Molnar, R.; Schlosser, G.; Cecal, A.; Drochioiu, G. *Isot. Environ. Health Stud.* **2007**, *43*, 105–116.
- (10) Rodriguez-Hernandez, J.; Babin, J.; Zappone, B.; Lecommandoux, S. *Biomacromolecules* **2005**, *6*, 2213–2220.
- (11) Haynie, D. T.; Zhang, L.; Rudra, J. S.; Zhao, W.; Zhong, Y.; Palath, N. *Biomacromolecules* **2005**, *6*, 2895–2913.
- (12) Kates, S. A.; Albericio, F. *Solid-Phase Synthesis*; Marcel Dekker, Inc.: New York, 2000.
- (13) Bush, A. I. *Curr. Opin. Chem. Biol.* **2000**, *4*, 184–191.
- (14) Benaki, D.; Zicos, C.; Evangelou, A.; Livanou, E.; Vlassi, M.; Mikros, E.; Pelecanou, M. *Biochem. Biophys. Res. Commun.* **2005**, *329*, 152–160.
- (15) Dobson, C. M. *Nature* **2002**, *418*, 729–730.
- (16) Pagel, K.; Vagt, T.; Kohajda, T.; Koksche, B. *Org. Biomol. Chem.* **2005**, *3*, 2500–2502.
- (17) Taylor, J. T.; Hardy, J.; Fischbeck, K. H. *Science* **2002**, *296*, 1991–1995.
- (18) Castano, E. M.; Prelli, F.; Wisniewski, T.; Golabek, A.; Kumar, R. A.; Soto, C.; Frangione, B. *Biochem. J.* **1995**, *306*, 599–604.
- (19) Hamazaki, H. *Biochem. Biophys. Res. Commun.* **1995**, *211*, 349–353.
- (20) Evans, K. C.; Berger, E. P.; Cho, C. G.; Weisgraber, K. H.; Lansbury, P. T., Jr. *Proc. Natl. Acad. Sci. U.S.A.* **1995**, *92*, 763–767.
- (21) Janciauskiene, S.; Garcia de Frutos, P.; Carlemalm, E.; Dahlback, B.; Eriksson, S. J. *Biol. Chem.* **1995**, *270*, 26041–26044.
- (22) Ma, Q. F.; Hu, J.; Wu, W. H.; Liu, H. D.; Du, J. T.; Fu, Y.; Wu, Y. W.; Lei, P.; Zhao, Y. F.; Li, Y. M. *Biopolymers* **2006**, *83*, 20–31.
- (23) Pang, D.; Yoo, S.; Dynan, W. S.; Jung, M.; Dritschilo, A. *Cancer Res.* **1997**, *57*, 1412–1415.
- (24) Yang, H.; Pritzker, M.; Fung, S. Y.; Sheng, Y.; Wang, W.; Chen, P. *Langmuir* **2006**, *22*, 8553–8562.
- (25) Merrifield, R. B. *J. Am. Chem. Soc.* **1963**, *85*, 2149–2154.
- (26) Chan, W. C.; White, P. D. *Fmoc Solid Phase Peptide Synthesis. A Practical Approach*; Oxford University Press, Inc.: New York, 2000.
- (27) Langer, R.; Peppas, N. A. *AIChE J.* **2003**, *49*, 2990–3006.
- (28) Chu, S. *Philos. Trans. R. Soc. London, Ser. A* **2003**, *361*, 689–698.
- (29) Wysocki, V. H.; Resing, K. A.; Zhang, Q. F.; Cheng, G. L. *Methods* **2005**, *35*, 211–222.
- (30) Souza, B. M.; Marques, M. R.; Tomazela, D. M.; Eberlin, M. N.; Mendes, M. A.; Palma, M. S. *Rapid Commun. Mass Spectrom.* **2004**, *18*, 1095–1102.
- (31) Souza, M. P.; Tavares, M. F. M.; Miranda, M. T. M. *Tetrahedron* **2004**, *60*, 4671–4681.
- (32) Pappalardo, G.; Impellizzeri, G.; Bonomo, R. P.; Campagna, G. G.; Saita, M. G. *New J. Chem.* **2002**, *26*, 593–600.

BM700793G